

Interaction between ultrasound and magnetization in ferromagnetic thin film studied by picosecond ultrasonics

ピコ秒超音波法を用いた強磁性薄膜中における超音波と磁化の相互作用の研究

Kakeru Tojo[‡], Akira Nagakubo^{*}, and Hirotsugu Ogi (Grad. School Eng., Osaka Univ.)
東條 翔[‡], 長久保 白^{*}, 荻 博次 (阪大大学院 工)

1. Introduction

The interaction between phonon and magnon (spin-wave, magnetic resonance, spin current, and so on) has attracted great attention. In particular, recent lithography techniques enable us to excite GHz-range surface acoustic waves (SAW), whose frequencies are close to those of the ferromagnetic resonance (FMR). A SAW with FEM frequency traveling along a ferromagnetic film is absorbed in the film when the applied magnetic field satisfies the FMR condition at a specific magnetic angle^{1,2}. SAW can be easily focused into an nm-region, which enables us to investigate the magnetic properties of single nanomagnets; previous studies use focused pulse light, leading to temperature increase. Actually, the smaller the nanomagnets' size, the larger the FMR amplitude³. However, SAW frequency is usually limited by ~ 10 GHz because of the IDT period.

Longitudinal ultrasound propagating in the thickness direction also can excite FMR. Bayer and co-authors succeeded in exciting 3–40 GHz FMR in magnetic film deposited on GaAs substrate by a strain pulse launched at the backsurface of the substrate using femtosecond lasers^{4–6}. A strain pulse excited in the magnetic film also leads to a magnetic response⁷, which can be enhanced by acoustic Bragg mirrors⁸. Sub-THz ultrasound can be used for investigating magnetic properties in a high-frequency range and the interaction between phonon and magnon. For further development of spintronics, it is important to understand them.

Therefore, in this study, we generate 10–100 GHz longitudinal ultrasound in Ni thin film using picosecond ultrasonics, and observe the magnetization by the time-resolved magneto-optical Kerr effect. We measure the angular dependence of the magnetization to evaluate the interaction between ultrasound and magnetization.

2. Measurement systems

We use picosecond ultrasonics which uses

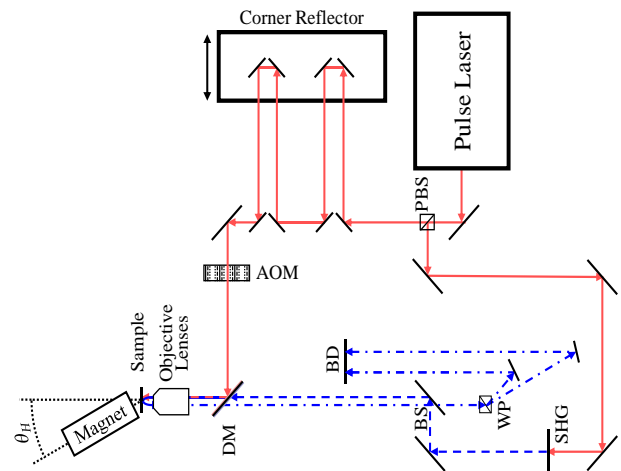


Fig. 1 Schematic of the optical systems. Red and Blue lines denote pump and probe light, respectively. The direction of the external magnetic field θ_H is defined as shown in the figure.

ultrafast laser pulses to excite and detect strain pulses. **Figure 1** shows a schematic of the optical systems we developed. We use a titanium-sapphire pulsed laser, whose repetition rate and center wavelength are 80 MHz and 800 nm, respectively. The pump and probe lights are separated by a polarization beam splitter (PBS). The difference in arrival time of them is adjusted by changing the optical path length by corner reflectors. The pump light is intensity-modulated at 100 kHz by an acousto-optic crystal modulator (AOM) for lock-in measurements. The pump light is reflected on a dichroic mirror (DM), so that the pump light is aligned with the probe light. Finally, the pump light enters the specimen through an objective lens.

The wavelength of the probe light is converted into 400 nm by a second harmonic generation (SHG) crystal, which is incident perpendicular to the specimen through the DM and objective lens. The probe light reflected from the specimen changes its polarization angle due to the Kerr effect, which is the Kerr-rotation angle. The

reflected light is separated into s- and p-polarized lights by a Wollaston prism (WP). The balanced detector (BD) outputs the intensity difference of them to a lock-in amplifier. The magnetization of the out-of-plane component of the specimen can be measured in a time-resolved.

3. Magnetization theory

We consider the magnetization dynamics in a ferromagnetic material under strain. Magnetization dynamics can be obtained by solving the Landau-Lifshitz-Gilbert equation from the following energies⁹⁾

$$E = -\mathbf{m} \cdot \mathbf{H} + K_d (\mathbf{m} \cdot \mathbf{n})^2 \quad (1)$$

where magnetization \mathbf{M} is normalized as $\mathbf{m} = \mathbf{M}/M_s$, by the saturation magnetization M_s , \mathbf{H} is magnetic field, $K_d = 2\pi M_s$ is the shape anisotropy and \mathbf{n} denotes a unit vector paralleled to the out-of-plane direction. The first and second terms represent the Zeman energy and the shape magnetic anisotropy energy, respectively. Assuming that the material is polycrystalline, the crystal magnetic anisotropy is ignored.

To represent the steady-state, we only need to consider the energy in **Eq. (1)**. When the strain pulse propagates, we also consider the magnetostriction energy of

$$E^m = b \varepsilon_{zz} m_z^2 \quad (2)$$

where b denotes the magnetoelastic coupling constants, ε_{zz} denotes the longitudinal-wave strain.

4. Results and discussion

The specimen is 300-nm Ni capped by 5-nm SiO₂ deposited on Si with a thermal oxide film. We show observed reflectivity changes in **Fig. 2**, which represents the strain changes near the surface. We observed echo signals every 95.4 ps, which agree with the round-trip time where 5.78-nm/ps ultrasound propagates in a 276-nm film.

We show the observed Kerr-rotation angle applying 0.5-T external magnetic field at $\theta_H = 20$ degrees in **Fig. 2**. This Kerr-rotation angle change represents the magnetization changes of the out-of-plane component. We observed about 16-GHz oscillation and pulse signal at ~95 ps. The oscillation corresponds to ferromagnetic resonance calculated by the Smit-Beljers formula¹⁰⁾, whose frequency changes with θ_H . On the other hand, the arrival time of the pulse signal at ~95 ps was the same for different θ_H , however, its amplitude changes. This echo signal in the Kerr-rotation angle is caused by the strain pulse. We will calculate the interaction between ultrasound and magnetization for different θ_H .

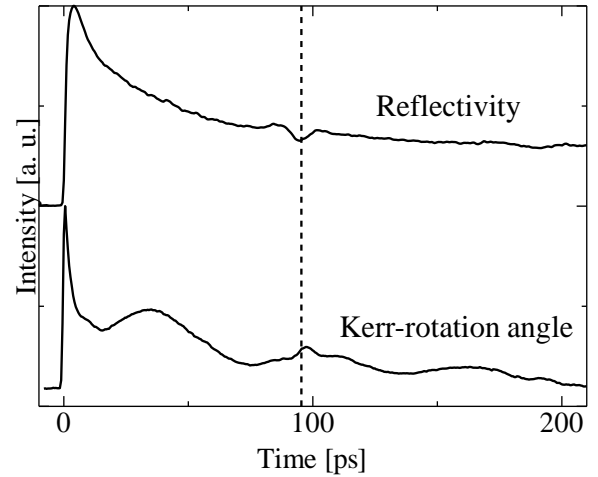


Fig. 2 Reflectivity changes and Kerr-rotation angle measured at $\theta_H = 20$ degrees. The value $t = 0$ corresponds to the time when the strain pulse is excited.

References

1. M. Weiler, L. Dreher, C. Heeg, H. Huebl, R. Gross, M. S. Brandt, and S. T. B. Goennenwein: Phys. Rev. Lett. **106** (2011) 117601.
2. L. Dreher, M. Weiler, M. Pernpeintner, H. Huebl, R. Gross, M. S. Brandt, and S. T. B. Goennenwein: Phys. Rev. B **86** (2012) 134415.
3. M. Jaris, W. Yang, C. Berk, and H. Schmidt: Phys. Rev. B **101** (2020) 214421.
4. A. V. Scherbakov, A. S. Salasyuk, A. V. Akimov, X. Liu, M. Bombeck, C. Brüggemann, D. R. Yakovlev, V. F. Sapega, J. K. Furdyna, and M. Bayer: Phys. Rev. Lett. **105** (2010) 117204.
5. M. Bombeck, A. S. Salasyuk, B. A. Glavin, A. V. Scherbakov, C. Brüggemann, D. R. Yakovlev, V. F. Sapega, X. Liu, J. K. Furdyna, A. V. Akimov, and M. Bayer: Phys. Rev. B **85** (2012) 195324.
6. J. V. Jäger, A. V. Scherbakov, T. L. Linnik, D. R. Yakovlev, M. Wang, P. Wadley, V. Holy, S. A. Cavill, A. V. Akimov, A. W. Rushforth, and M. Bayer: Appl. Phys. Lett. **103** (2013) 032409.
7. J. Kim, M. Vomir, and J. Bigot: Phys. Rev. Lett. **109** (2012) 166601.
8. J. V. Jäger, A. V. Scherbakov, B. A. Glavin, A. S. Salasyuk, R. P. Champion, A. W. Rushforth, D. R. Yakovlev, A. V. Akimov, and M. Bayer: Phys. Rev. B **92** (2015) 020404.
9. Y. Yahagi, C. Berk, B. Hebler, S. Dhuey, S. Cabrini, M. Albrecht and H. Schmidt: J. Phys. D: Appl. Phys. **50** (2017) 17LT01.
10. S.V. Vonsovskii, Ferromagnetic Resonance, Pergamon, Oxford, (1966).